Operating Modes of a Teetered-Rotor Wind Turbine

Gunjit S. Bir
National Wind Technology Center
National Renewable Energy Laboratory

Karl Stol
University of Colorado at Boulder

NREL

NOTICE

Available to DOE and DOE contractors from:
Office of Scientific and Technical Information (OSTI)
P.O. Box 62
Oak Ridge, TN 37831
Prices available by calling (423) 576-8401

Available to the public from:
National Technical Information Service (NTIS)
U.S. Department of Commerce
5285 Port Royal Road
Springfield, VA 22161
(703) 487-4650

Printed on paper containing at least 50% wastepaper, including 20% postconsumer waste

OPERATING MODES OF A TEETERED-ROTOR WIND TURBINE

Gunjit Bir[†] and Karl Stol[*]

[†]National Renewable Energy Laboratory
National Wind Technology Center
1617 Cole Boulevard, Golden, CO 80401-3393

[*]Department of Aerospace Engineering Science
University of Colorado at Boulder, Boulder, CO 80309-0429

Abstract

We examine the operating modes of a two-bladed teetered wind turbine. Because of the gyroscopic asymmetry of its rotor, this turbine's dynamics can be quite distinct from those of a turbine with three or more blades. This asymmetry leads to system equations with periodic coefficients that are solved using the Floquet approach to extract the correct modal parameters. The system equations are derived using a simple analytical model with four degrees of freedom: nacelle yaw, rotor teeter, and flapping associated with each blade. Results confirm that the turbine modes become more dominated by the centrifugal and gyroscopic effects as the rotor speed increases. The gyroscopic effect may also cause dynamic instability. Under certain design conditions, yaw and teeter modal frequencies may coalesce.

Introduction

Traditionally, modes of a wind turbine are computed with its rotor in a parked (non-operating) condition. While such modes help validate a turbine's structural properties, they do not capture the dominant centrifugal and gyroscopic effects associated with an operating rotor. Operating modes play a key role in identifying the mechanisms that cause adverse loads and designing controls to improve stability and loads. Because of the complexity of dynamic behavior of wind turbines, consisting of rotating components coupled to stationary components, only limited attempts [1-8] have been made to compute operating turbine modes. All these attempts used time-intensive simulations and post-processing of time response data to extract modal frequencies and treated the turbine as a time-invariant system.

An earlier paper [8] presented the operating modes of a three-bladed wind turbine. Because of the structural asymmetry associated with a three-bladed rotor, a multi-blade coordinate transformation [9] was sufficient to transform the time-periodic equations into a set of time-invariant governing equations and therefore conventional modal identification techniques sufficed.

However, modes were identified from time-intensive post-processing of several simulations. A new wind turbine code is under development [10] that would provide comprehensive aeroelastic models of the full turbine system in explicit forms required for direct modal analysis. It will be some time before this code is developed and validated. Meanwhile, Stol [11] has developed a simple model with $5+N_b$ degrees of freedom, where N_b is the number of blades. This model is briefly described in the next section; it idealizes the wind turbine structure as an assemblage of rigid bodies interconnected by springs and joints. Though it does not model all the flexibility effects, it does capture the dominant physics of a rotating wind turbine.

For modal analysis of a two-bladed teetered-rotor turbine, which is the focus of this paper, we use only those four degrees of freedom that are essential to capturing system dynamics without added complexity. We reduce the $5+N_b$ degree-of-freedom model, mentioned earlier, to the desired four-degree-of-freedom model by locking the degrees of freedom not relevant to our teetered turbine. The governing system equations clearly show time-periodic terms as expected of a two-bladed rotor whose gyroscopic properties undergo a periodic variation with each rotor revolution. Since the governing equations are periodic, a conventional eigenanalysis yields erroneous results. Therefore, we use Floquet analysis, briefly described in a following section, to compute the modal properties. Results are presented for three models: a single-yaw-degree-of-freedom model (teetered and flapping of blades locked), a yaw-and-teeter-degree-of-freedom model (flapping of blades locked), and the full four-degree-of-freedom model.

Analytical Model

Figure 1 shows a schematic of the wind turbine used for analytical modeling. It is idealized as an assemblage of rigid bodies, i.e., tower, bed frame, nacelle, generator lumped with the high-speed shaft, low-speed shaft, hub, and the blades, interconnected by revolute joints. Each revolute joint allows one degree of freedom, which is a

measure of the relative angular displacement between the two adjacent components it joins. A complete list of the degrees of freedom and the geometric parameters that define the turbine configuration is also provided in the figure. A spring or a damper may restrain each joint. A flap spring is added to model the blade-distributed flap flexibility lumped at the flap hinge. A spring may be placed between the low-speed and high-speed shafts to model the drivetrain flexibility. Aerodynamic loading is ignored, but the gravity effects are included. Complete modeling details, derivation of the analytical model, and the validation attempts, are provided in Ref [11]. The analytical model was derived using Lagrange's energy approach in conjunction with the Danavit-Hartenberg convention [12] for defining system kinematics.

Our two-bladed, teetered-rotor turbine has no tilt degree of freedom. Its rotor speed is assumed constant; this amounts to assuming a rigid rotor shaft and a constant-speed synchronous generator. We therefore lock out the tilt and the rotor shaft compliance degrees of freedom in the aforementioned analytical model. The resulting four-degree-of-freedom model is linearized about the steady operating state of the turbine. We assume a steady operating state in which all the degrees of freedom except the rotor azimuth have zero values. This leads to a very simplified set of linearized equations, presented in the Appendix in a matrix form. The vector of unknowns comprises the four degrees of freedom, i.e., the yaw angle γ, the teeter angle ϕ, the flapping angle β_1 for blade 1, and the flapping angle β_2 for blade 2. The inertia, gyroscopic, and stiffness

matrices depend on the rotor azimuth position, ψ, and the turbine geometric, mass, stiffness, and damping properties listed in Table 1. Note that the gyroscopic matrix is multiplied by Ω, the rotor speed, and the stiffness matrix is multiplied by Ω^2. The stiffness matrix also depends on the gravity, g. For a constant rotor speed, $\psi = \Omega t$. The governing equations are therefore periodic in time with period $T = 2\pi / \Omega$. Physical interpretation of all the terms appearing in these matrices is outside the intent of this paper. However, a few observations follow. All the gyroscopic terms, which of course exclude the structural damping terms that appear on the diagonal of the gyroscopic matrix, cross couple the degrees of freedom. This implies, owing to rotor rotation, a motion in one degree of freedom would induce a gyroscopic motion in another degree of freedom. An exception to this is the direct gyroscopic term, $g_{\gamma\gamma}$. A yaw motion of the nacelle causes the two-bladed rotor also to yaw, and this induces a gyroscopic moment about the tower yaw axis. This term would not appear if we had gyroscopic symmetry associated with three or more blades. The important point to note is that this self-induced gyroscopic moment is a multiple of $\sin 2\psi$ and therefore shows 2p variation, where p denotes *per rotor revolution*. All the other terms in the matrix represent gyroscopic cross coupling and show a 1p variation. We also note that the flap and teeter motions are gyroscopically decoupled. This is because both these motions occur about parallel axes and are referenced to the same hub-fixed rotating frame.

Degrees-of-freedom
γ Bed-plate yaw angle
τ Nacelle tilt angle
ψ Rotor shaft (*azimuth*) angle
ψ_g Rotor shaft compliance angle
ϕ Hub teeter angle
β_1 Blade #1 flap angle
β_2 Blade #2 flap angle

Geometric constants
a   Yaw pivot to tilt pivot distance
b   Tilt pivot to shaft axis distance
d   Tilt pivot to hub distance
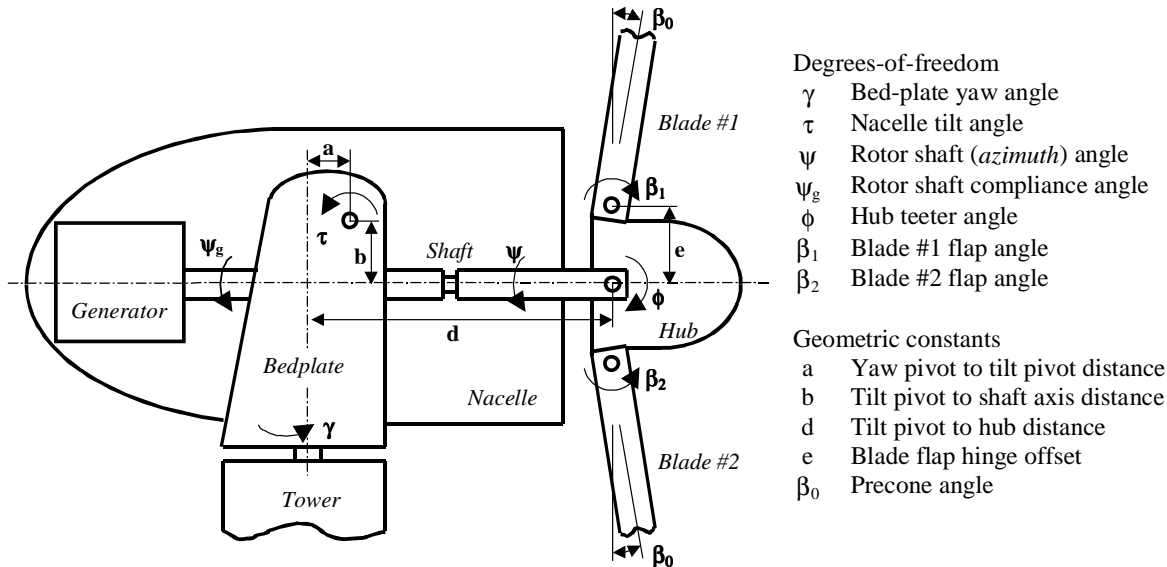e   Blade flap hinge offset
β_0 Precone angle

Fig. 1. Wind turbine schematic showing degrees of freedom and geometric parameters.

Floquet Approach

For modal analysis, we first transform the linearized matrix equation shown in the Appendix to a first-order form:

$$\dot{\mathbf{y}} = A(t)\mathbf{y} \qquad (1)$$

where the state vector is defined as

$$\mathbf{y} = \begin{bmatrix} \gamma & \phi & \beta_1 & \beta_2 & \dot{\gamma} & \dot{\phi} & \dot{\beta}_1 & \dot{\beta}_2 \end{bmatrix}^T$$

and $A(t)$ is the system time-periodic matrix given in terms of the inertia matrix $M(t)$, gyroscopic matrix $C(t)$, and the stiffness matrix $K(t)$:

$$A(t) = \begin{bmatrix} 0 & I_{4X4} \\ -M^{-1}K & -M^{-1}C \end{bmatrix} \qquad (2)$$

According to Floquet theory [9,13], the solution of eq. (1) can be expressed as

$$\mathbf{y}(t) = P(t)\Lambda(t)\mathbf{c} \qquad (3)$$

where $P(t)$ is a periodic matrix, $\mathbf{c}$ is a vector of arbitrary constants, and $\Lambda(t)$ is a diagonal matrix whose i^{th} diagonal term is

$$\Lambda_i(t) = e^{s_i t} \qquad (4)$$

From eq. (3), the solution at time $t = 0$ is

$$\mathbf{y}(0) = P(0)\mathbf{c} \qquad (5)$$

and, in view of the fact that $P(t)$ is periodic, the solution at time $t = T$ is

$$\mathbf{y}(T) = P(T)\Lambda(T)\mathbf{c} = P(0)\Lambda(T)\mathbf{c} \qquad (6)$$

We now define the system transition matrix Φ as a matrix relating the solutions of eq. (1) at time $t = 0$ and time $t = T$ as follows

$$\mathbf{y}(T) = \Phi\mathbf{y}(0) \qquad (7)$$

Substituting eqs. (5) and (6) in (7), we obtain

$$[P(0)\Lambda(T) - \Phi P(0)]\mathbf{c} = 0 \qquad (8)$$

Because $\mathbf{c}$ is arbitrary, the above equation implies

$$\Phi P(0) = P(0)\Lambda(T) \qquad (9)$$

If Φ is known, eq. (9) can be solved as an eigenvalue problem to yield the eigenvalues matrix $\Lambda(T)$ and the eigenvectors matrix $P(0)$. According to eq. (4), the characteristic exponent is given by

$$s_i = \varsigma_i + j\omega_i$$
$$= \frac{1}{T}\ln|\Lambda_i| + j\frac{1}{T}\tan^{-1}\frac{\text{Re}(\Lambda_i)}{\text{Im}(\Lambda_i)} \qquad (10)$$

where j equals $\sqrt{-1}$. In view of the foregoing development, the Floquet approach for modal analysis comprises the following three steps:

- *Compute the transition matrix Φ.* Choose N linearly independent initial conditions $Y(0) = I_{NXN}$, where N represents dimension of the state vector. Integrate eqs (1) for each column of the initial conditions to compute $Y(T)$. In view of eq. (7), $\Phi = Y(T)$.

- *Compute the eigenvalues $\Lambda(T)$ of the transition matrix* using any standard software package.

- *Compute modal dampings and frequencies.* In view of eq. (10), the modal damping is given by

$$\varsigma_i = \frac{1}{T}\ln|\Lambda_i|$$

and the modal frequency is given by

$$\omega_i = \frac{1}{T}\tan^{-1}\frac{\text{Re}(\Lambda_i)}{\text{Im}(\Lambda_i)}$$

Results and Discussion

As mentioned earlier, we model the turbine as a four-degree-of-freedom system. These degrees of freedom comprise nacelle yaw, hub teeter, and flapping of the two blades. Before analyzing the modal behavior of this model, we consider two simple cases. In the first case, we allow only the yaw degree of freedom (the rotor of course is spinning at a constant rate). In the second case, we allow the hub teeter motion as well. For each case, we use the structural and configuration parameters listed in Table 1 to build our turbine model.

Case I: Turbine with only Yaw Degree of Freedom

We first try conventional modal analysis on this model (yaw spring and damper are removed to further simplify the model). Since the governing equation is second

Symbol	Description	Value
Ω_0	Nominal shaft rotation rate	6.02 rad/s (57.5 rpm)
τ	Nacelle tilt angle	0°
β_0	Precone angle	7°
a	Longitudinal distance from yaw pivot to tilt pivot	0 m
b	Vertical distance from tilt pivot to shaft axis	0 m
d	Longitudinal distance from tilt pivot to hub (overhang)	2.388 m
e	Flap-hinge offset	0.28 m
c_b	Center of mass distance of blade from hinge	4.21 m
m_b	Mass of each blade	569 kg
I_{yaw}	Moment of inertia about the yaw axis (excludes blades)	16 599 kgm^2
I_b	Moment of inertia of blade about flap hinge	16 857 kgm^2
$I_{b\text{-long}}$	Moment of inertia of blade about longitudinal (pitch) axis	5 kgm^2
$I_{h\text{-lat}}$	Moment of inertia of hub about a lateral axis	50 kgm^2
$I_{h\text{-long}}$	Moment of inertia of hub about the spin axis	5 kgm^2
K_{yaw}	Yaw spring stiffness	573 Nm/rad
K_{teeter}	Teeter spring stiffness	573 Nm/rad
K_{flap}	Flap spring stiffness	358 200 Nm/rad

Table 1. Structural and geometric properties of the two-bladed wind turbine.

order in yaw, γ, we get two eigenvalues. One eigenvalue is zero implying undamped rigid body yaw mode; the other eigenvalue has a zero imaginary part, implying zero frequency, and an azimuth-dependent real part, implying a time-varying damping. Figure 2 shows the azimuth-dependent real part, normalized with respect to the rotor speed (henceforth, all the eigenvalues will be shown normalized with respect to the rotor speed). The yaw damping shows a 2p variation (p denotes *per rotor revolution*). We may be tempted to interpret this as a periodic loss and gain of the nacelle kinetic energy to the rotor. This is because the rotor angular momentum about the yaw axis is conserved and its yaw angular velocity must vary to accommodate the 2p variation of its inertia about the yaw axis. This causes 2p variation in the rotor kinetic energy. The nacelle responds by varying its yaw

velocity to keep the total system energy constant. We shall soon see that the total system energy is in fact conserved and the overall system damping is zero for any time instants. The direct eigenanalysis therefore yields erroneous results. Even the exchange of kinetic energy between the nacelle and the rotor is not correctly captured by the damping variation shown in the figure.

We now try the Floquet approach noting that the governing equation is periodic in the rotor azimuth position, ψ. Since ψ equals Ωt, the azimuth in fact represents non-dimensionalized time. Floquet analysis yields two zero eigenvalues implying two rigid body modes, both undamped. The first mode is a constant-yaw-position rigid body mode, and the other mode is a constant-yaw-velocity rigid body motion modulated by a time-periodic modal amplitude. The modal amplitude
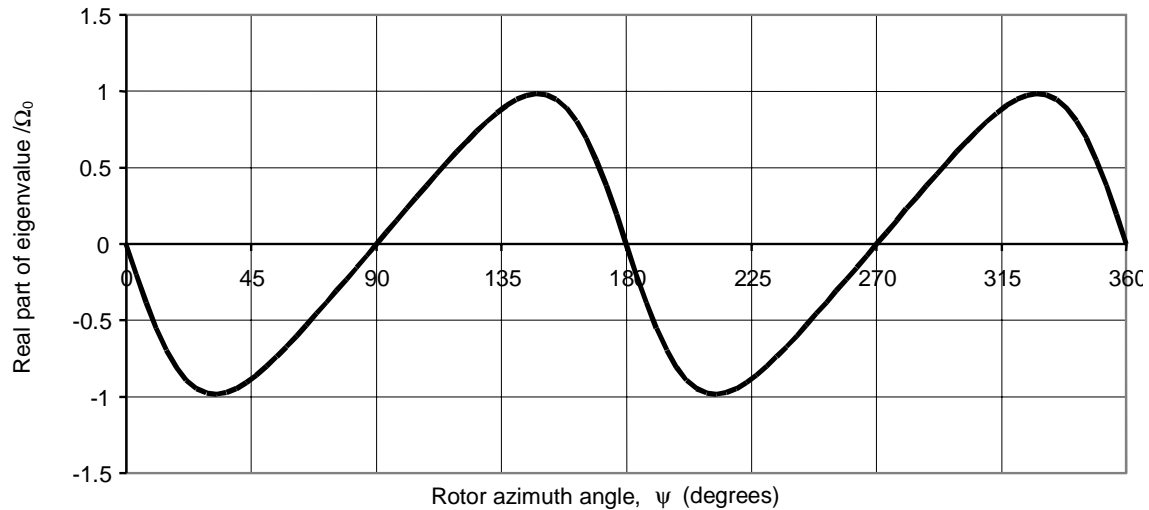

Fig. 2. Conventional-modal-analysis-predicted yaw modal damping variation with rotor azimuth (nominal rotor speed, Ω_0=57.5 rpm).
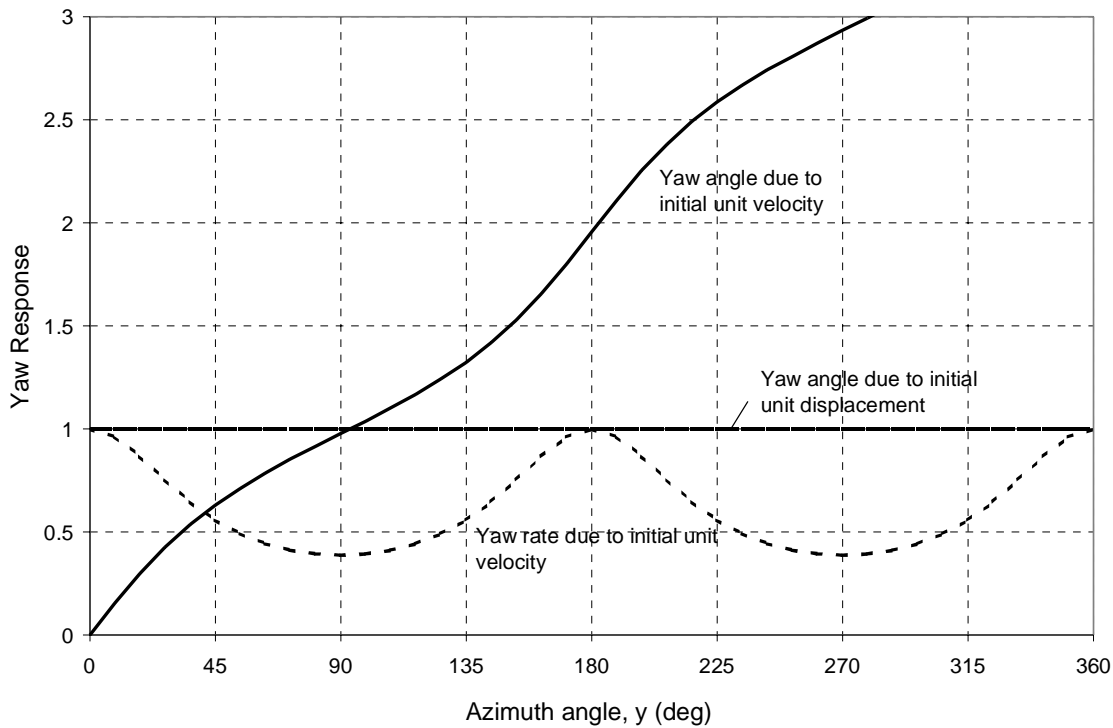
Fig. 3. Yaw response due to initial conditions (turbine model with yaw degree of freedom only).

can be identified with $P(t)$ in eq. (3). To confirm Floquet analysis results, we look at yaw response histories due to two sets of initial conditions. The first set of initial conditions, a unit yaw position and a zero yaw velocity, results in a constant-yaw-position response (see Figure 3). This corresponds to the first rigid body mode. The second set of initial conditions, a zero yaw position and a unity yaw velocity, results in a constant-yaw velocity response with a 2p variation superimposed on it. This 2p variation is the result of the direct gyroscopic term, $g_{\gamma\gamma}$, described earlier. Also, both the position and velocity response histories in the figure show zero damping. Floquet analysis therefore yields correct modal properties and we use it to obtain all the subsequent results.

Case II: Turbine with only Yaw and Teeter Degrees of Freedom

This represents a fourth-order system. All spring and damping values are again assumed zero. Floquet analysis of this system yields four eigenvalues:

$$\begin{pmatrix} 0 & 0 & 0.0476+ j1.0 & -0.0476- j1.0 \end{pmatrix}$$

The first two zero eigenvalues correspond to the rigid-body yaw modes. The third eigenvalue corresponds to a teeter-yaw mode in which teeter motion is coupled with an in-phase yaw motion. The mode associated

with the fourth eigenvalue is exactly like the third mode except that the yaw motion participation is out of phase with the teeter motion. The interesting point to note is that, unlike a set of complex conjugate eigenvalues characterizing a conventional system, the third and fourth eigenvalues have their real parts also of opposite sign. The third eigenvalue, with a positive real part, implies instability, and the fourth eigenvalue, with a negative real part, implies stability. A gyroscopic system can exhibit this type of self-excited instability. The energy that causes this instability, i.e., divergent teeter oscillation, comes from the rotor rotational kinetic energy about its shaft. The rotor speed, if allowed to vary, would drop in response to the energy drawn by the divergent teeter motion and instability would be arrested. Constant rotor speed implies that the induction generator behaves as a motor, draws energy from the electric grid, and feeds it to the rotor. It should be pointed out that the aerodynamic forces, which we have neglected, could drastically alter the system damping levels, if not the frequencies.

We now examine the system response due to four sets of initial conditions: unity yaw displacement alone, unity yaw velocity alone, unity teeter displacement alone, and unity teeter velocity alone. An initial unit yaw displacement causes participation of only the first rigid-body yaw mode, and the system remains in the same displaced state (figure not shown). Each of the other three sets of initial conditions causes participation
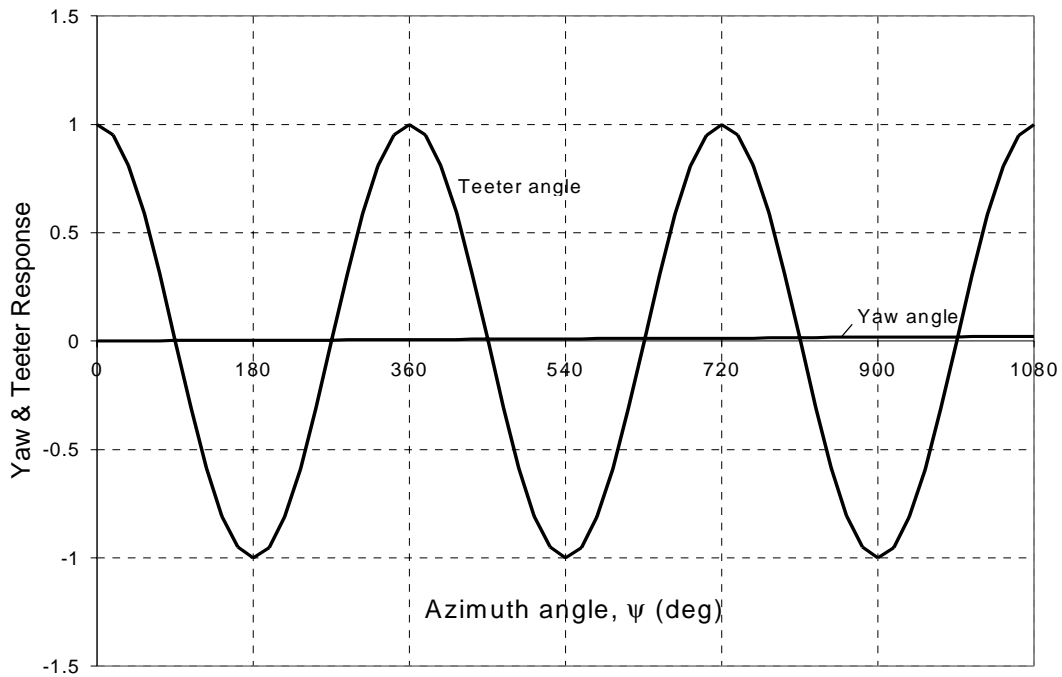
Fig. 4a. Yaw and teeter response due to an initial unit teeter displacement (turbine model with yaw and teeter degrees of freedom only).

of all the modes, including the unstable teeter mode. The relative participation of different modes of course depends on the initial condition. Figures 4a-4c show teeter and yaw responses due to these three initial conditions. Note that all the responses are unstable; this is due to the participation of the third coupled teeter-yaw mode.

Case III: The Four-Degree-of-Freedom Turbine Model

This represents an eighth-order periodic system. The joint springs, gravity, and precone are reintroduced in this model. At the rotor nominal speed, Ω_0=57.5 rpm, the Floquet analysis yields two real eigenvalues and six complex eigenvalues:
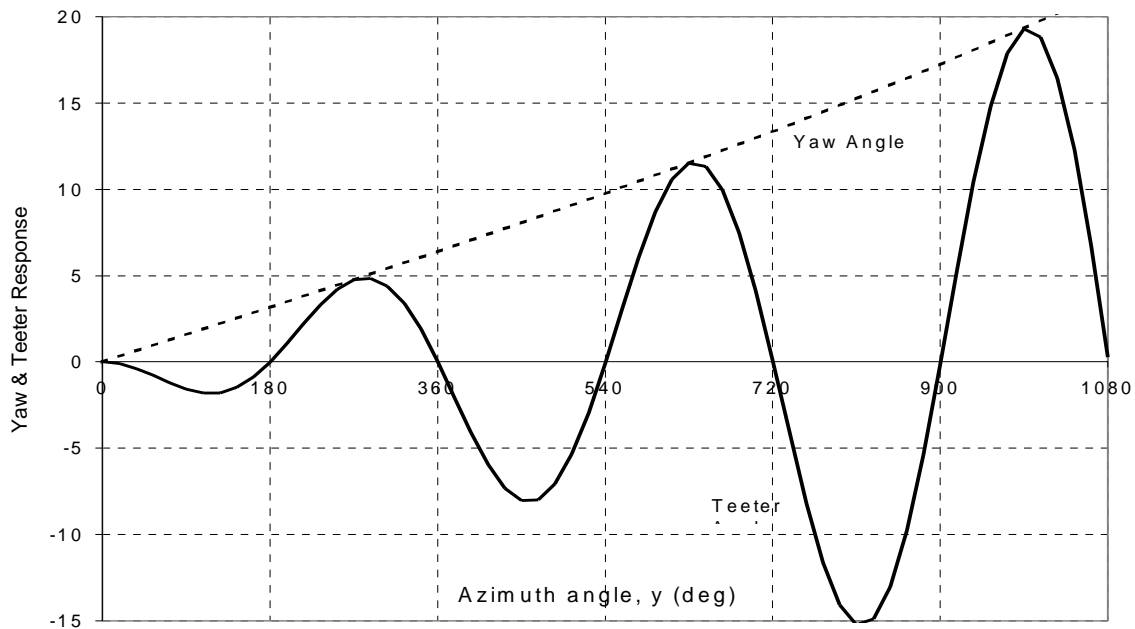

Fig. 4b. Yaw and teeter response due to an initial unit yaw velocity (turbine model with yaw and teeter degrees of freedom only).
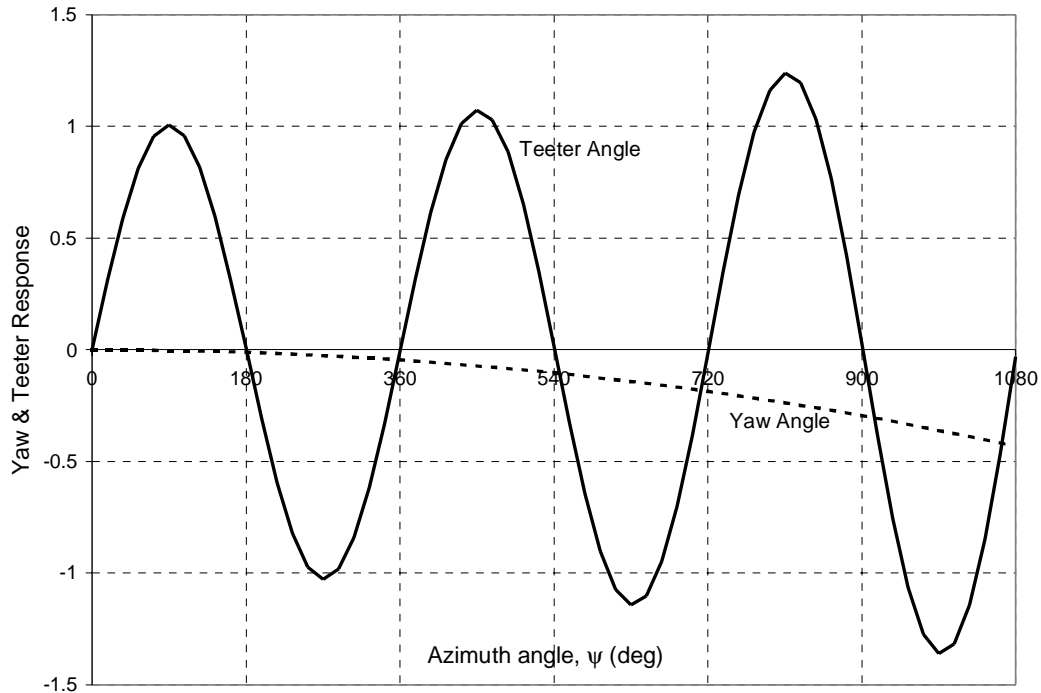
Fig. 4c. Yaw and teeter response due to an initial unit teeter velocity (turbine model with yaw and teeter degrees of freedom only).

$(\pm 0.00096, \pm 0.0415 \pm j1.0, \pm j1.0196, \pm j14.1029)$

The first pair of real eigenvalues represents two rigid-body yaw modes, one marginally damped and the other marginally unstable. The second complex pair of eigenvalues represents two coupled teeter-yaw modes having the same 1p frequency, but opposite damping levels. The third complex pair corresponds to the collective flap mode in which the two blades flap in phase. The fourth pair corresponds to the differential
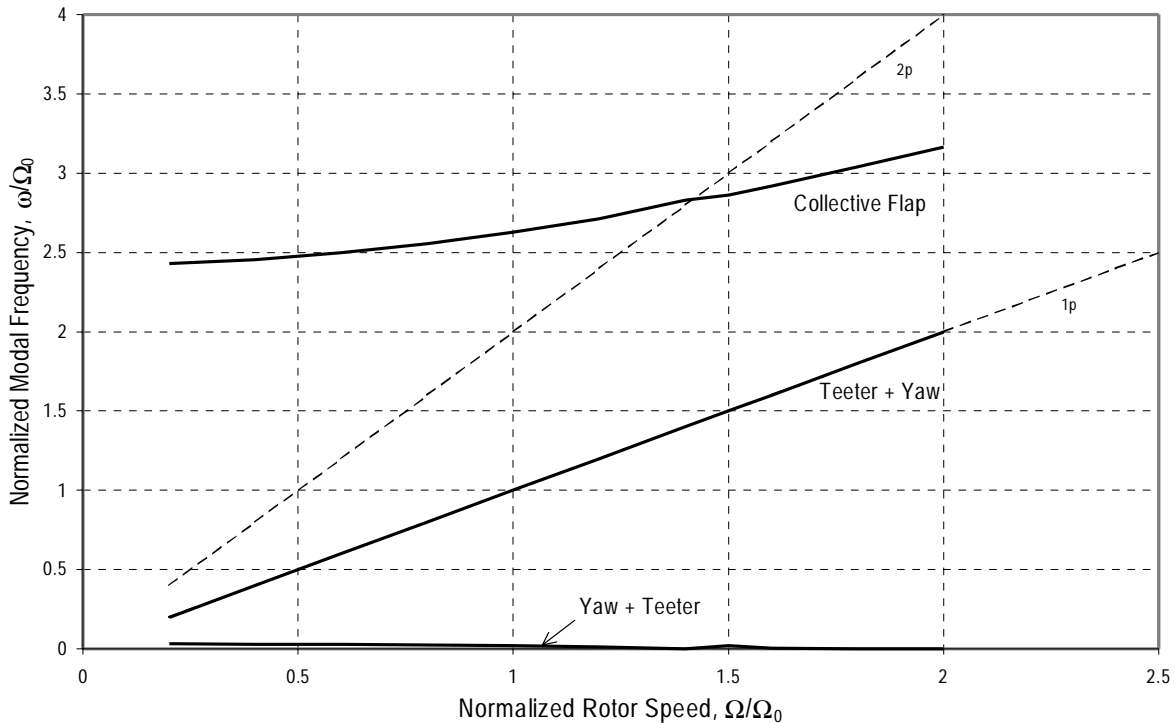

Fig. 5. Operating modal frequencies for the four-degree-of-freedom turbine model (Ω_0=57.5 rpm).
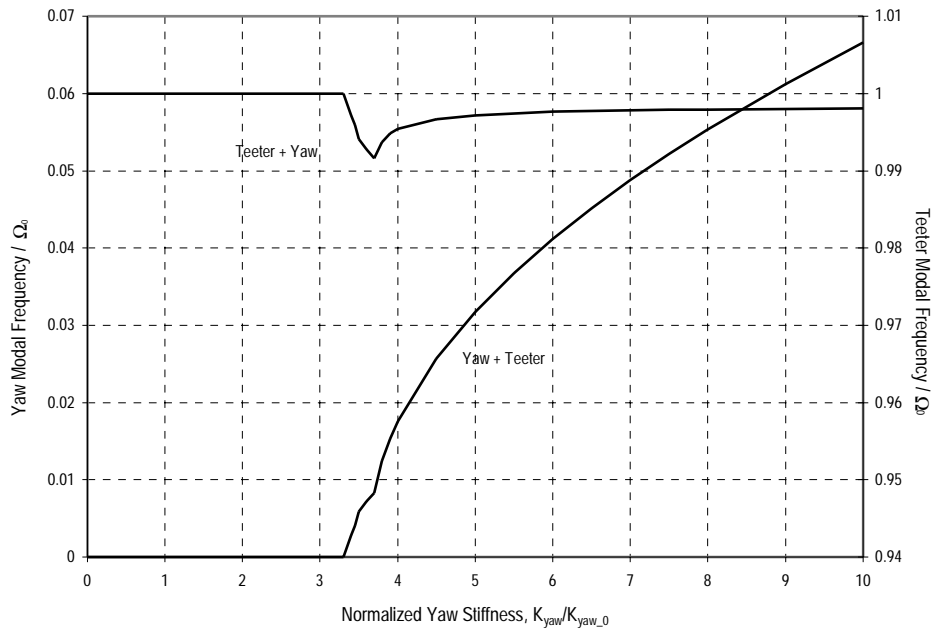
Fig. 6a. Effect of yaw stiffness on modal frequencies (nominal stiffness, $K_0 = 570$ Nm/rad)

flap mode wherein the blades flap differentially, i.e., out of phase; this differential flapping is coupled with a significant hub teeter motion. The collective flap frequency is predominantly dictated by the centrifugal stiffening effect associated with the $K_{\beta\beta}$ term in the stiffness matrix (see Appendix). The differential mode is determined by the oscillation of the hub while resisting the centrifugal pulling by the two blades.

Figure 5 shows the effect of rotor speed on the modal frequencies. The collective flap frequency increases with rotor speed because of the centrifugal stiffening effect and asymptotically tends towards 1p. Not shown in the figure is the differential flap frequency, which also increases with the rotor speed. The teeter mode
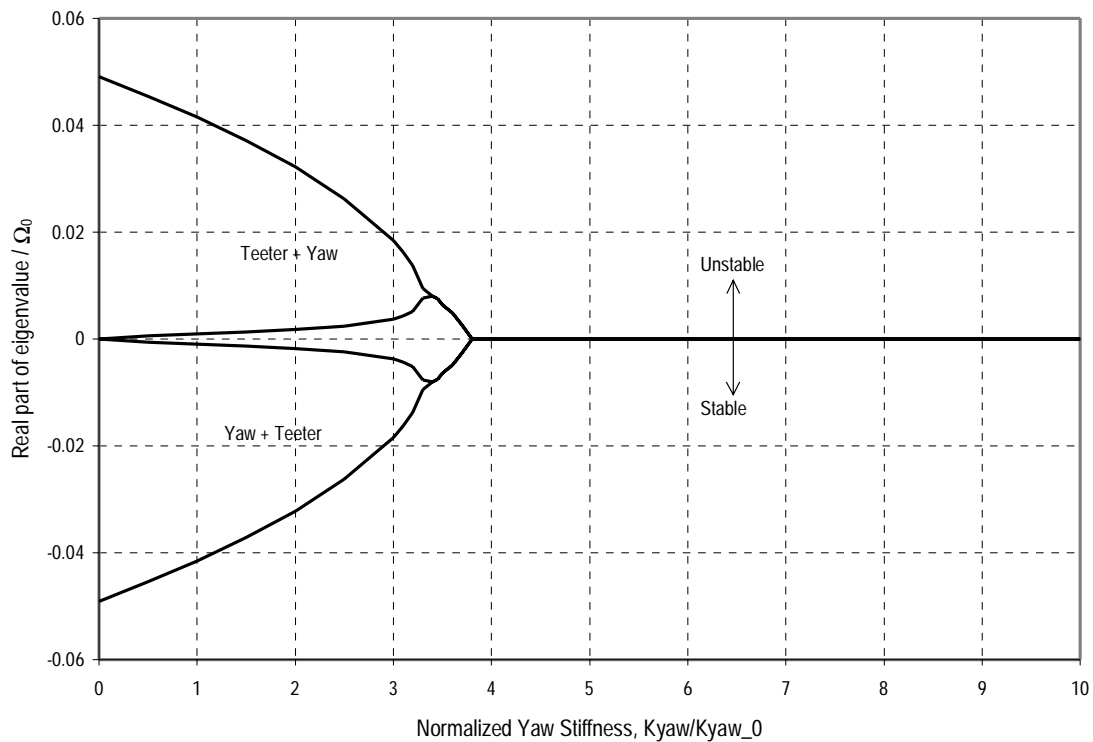

Fig. 6b. Effect of yaw stiffness on modal damping (nominal stiffness, $K_0 = 570$ Nm/rad)

frequency follows the 1p trend and the yaw mode frequency stays close to zero.

Figure 6 shows the results of a typical parametric study wherein the yaw stiffness is varied from a zero value to a value ten times the nominal stiffness. Results are somewhat counter-intuitive. Figure 6a shows that for yaw stiffness values below the $3.3K_{yaw0}$ level, the yaw frequency remains zero despite increasing yaw stiffness. This is because the rotor gyroscopic forces rather than the low yaw spring force control the yaw dynamics. The rotor teeters at a frequency of 1p, when observed from the hub-attached rotating frame. The nacelle, the motion of which is defined with respect to the ground-fixed frame, experiences this as a 0p and 2p forcing. This causes a zero-frequency yaw mode modulated by a 2p frequency, just as pointed out under Case I. Beyond the $3.3K_{yaw0}$ value, the yaw spring force dominates the gyroscopic coupling effect and therefore the yaw frequency tends to increase. The nacelle yaw frequency, ω_γ is seen in the rotor frame as a $1p \pm \omega_\gamma$ frequency. The $1p - \omega_\gamma$ motion of the nacelle couples with the hub teeter dynamics and causes a reduction in the teeter frequency. Thus, the nacelle yaw motion, as observed in the rotating frame, is locked with teeter motion and remains so until K_{yaw} exceeds 3.7 times the nominal stiffness. Beyond this value, the yaw stiffness almost exclusively controls the yaw frequency and the teeter frequency tends to revert back to the 1p value. Figure 6b shows that for low yaw stiffness values, wherein the gyroscopic effects dominate, both the teeter and the yaw modes exhibit instability (associated with positive real parts of their corresponding eigenvalues). After K_{yaw} exceeds 3.7 times the nominal yaw stiffness value, the yaw-spring dominates the gyroscopic coupling effects and the damping levels fall to zero.

Concluding Remarks

Modal behavior of a two-bladed wind turbine, modeled as a simple four-degree-of-freedom system, was analyzed. We established that the time-periodic governing equations mandate a Floquet analysis. Results showed that centrifugal stiffening dictates the rotor flap modes, whereas gyroscopic effects control the yaw and teeter modes. The gyroscopic effects may cause instability. We also showed that, under certain design conditions, two modes might coalesce at a single frequency.

Our studies ignored flexibility and aerodynamic effects. A code is under development that will include these effects as well as other degrees of freedom like the tower deflections and the blade inplane and twist defections. The Floquet analysis will also be extended to handle an aeroelastic system with a large number of degrees of freedom.

Acknowledgements

References

[1] James, G.H., "Extraction of Modal Parameters from an Operating HAWT using the Natural Excitation Technique (NExT)", *Proceedings of the 1994 ASME Wind Energy Symposium, Wind Energy-1994, SED-Vol. 15*, New York: American Society of Mechanical Engineers; pp. 227-232.

[2] Malcolm, D.J.; James, G.H., "Identification of Natural Operating Modes of HAWTs from Modeling Data", *Proceedings of the 1996 Wind Energy Symposium, Wind Energy, Vol. 1*, New York, NY: American Society of Mechanical Engineers, 1996, pp. 24-31.

[3] Lobitz, D.W., Sullivan, W.N. *VAWTDYN: A Numerical Package for the Dynamic Analysis of Vertical Axis Wind Turbine*, Report SAND-80-0085, Albuquerque, NM: Sandia National Laboratories, July 1980.

[4] Carne, T.G.; Lobitz, D.W.; Nord, A.R.; Watson, R.A., "Finite Element Analysis and Modal Testing of a Rotating Wind Turbine", Presented at the *AIAA/ASME/ASCE/AHS Structures - Structural; Dynamics and Materials Conference*, New Orleans, LA, May 9, 1982.

[5] Carne, T.G.; Martinez, D.R.; Ibrahim, S.R. *Modal Identification of a Rotating Blade System,* Report SAND82—2115 UC--32, Albuquerque, NM: Sandia National Laboratories, October 1991.

[6] James, G.H.; Carne, T.G.; Lauffer J.P. *The Natural Excitation Technique (NExT) for Modal Parameter Extraction from Operating Wind Turbines*, Report SAND92—1666, UC--261, Albuquerque, NM: Sandia National Laboratories, February 1993.

[7] Yamane, T., Thresher, R.W., "Coupled Rotor/Tower Stability Analysis of a 6-meter Experimental Wind Turbine", Presented at *the Sixth ASME Wind Energy Symposium,* Dallas, TX, February 1987.

[8] Bir, G.S., Butterfield, C.P., "Modal Dynamics of a Next-Generation Flexible-Rotor Soft-Tower Wind Turbine", *Proceedings of the 15th International Modal Analysis Conference*, Orlando, Florida, 1997.

[9] Johnson, W.J., *Helicopter Theory,* Princeton, NJ: Princeton University Press, 1980.

[10] Bir, G.S., Robinson, M., "Code Development for Control Design Applications (Phase I: Structural Modeling)", *Proceedings of the 18th AIAA/ASME Wind Energy Symposium*, Reno, Nevada, January 11-14, 1999.

[11] Stol, K., Bir, G.S., Balas, M., "Linearized Dynamics and Operating Modes of a Simple Wind Turbine Model", *Proceedings of the 18th AIAA/ASME Wind Energy Symposium*, Reno, Nevada, January 11-14, 1999.

[12] Devavit, J., Hartenberg, R.S., "A Kinematic Notation for Lower-Pair Mechanisms Based on Matrices", *ASME J. Applied Mechanics, No. 2*, 1955, pp. 215-221.

[13] Nayfeh, A.H., Mook, D.T., *Nonlinear Oscillations*, John Wiley & Sons, New-York, 1979.

Appendix

The linearized equations for the four-degree-of-freedom turbine model are:

$$\begin{bmatrix} m_{\gamma\gamma} & m_{\gamma\phi} & m_{\gamma\beta_1} & m_{\gamma\beta_2} \\ m_{\phi\gamma} & m_{\phi\phi} & m_{\phi\beta_1} & m_{\phi\beta_2} \\ m_{\beta_1\gamma} & m_{\beta_1\phi} & m_{\beta_1\beta_1} & 0 \\ m_{\beta_2\gamma} & m_{\beta_2\phi} & 0 & m_{\beta_2\beta_2} \end{bmatrix} \begin{Bmatrix} \ddot{\gamma} \\ \ddot{\phi} \\ \ddot{\beta}_1 \\ \ddot{\beta}_2 \end{Bmatrix} + \Omega \begin{bmatrix} g_{\gamma\gamma} & g_{\gamma\phi} & g_{\gamma\beta_1} & g_{\gamma\beta_2} \\ g_{\phi\gamma} & g_{\phi\phi} & 0 & 0 \\ g_{\beta_1\gamma} & 0 & g_{\beta_1\beta_1} & 0 \\ g_{\beta_2\gamma} & 0 & 0 & g_{\beta_2\beta_2} \end{bmatrix} \begin{Bmatrix} \dot{\gamma} \\ \dot{\phi} \\ \dot{\beta}_1 \\ \dot{\beta}_2 \end{Bmatrix} + \Omega^2 \begin{bmatrix} k_{\gamma\gamma} & k_{\gamma\phi} & k_{\gamma\beta_1} & k_{\gamma\beta_2} \\ 0 & k_{\phi\phi} & k_{\phi\beta_1} & k_{\phi\beta_2} \\ 0 & k_{\beta_1\phi} & k_{\beta_1\beta_1} & 0 \\ 0 & k_{\beta_2\phi} & 0 & k_{\beta_2\beta_2} \end{bmatrix} \begin{Bmatrix} \gamma \\ \phi \\ \beta_1 \\ \beta_2 \end{Bmatrix} = \{0\}$$

where $\gamma, \phi, \beta_1, \beta_2$ denote the yaw, teeter, blade-1 flap, and blade-2 flap degrees of freedom, respectively. To express entries in the inertia, gyroscopic, and stiffness matrices, we use the following notation:

$$S = \sin\psi$$
$$C = \cos\psi$$
$$k_q = \text{torsion stiffness in the } q^{th} \text{ degree of freedom}$$
$$\bar{c}_q = \text{torsion damping in the } q^{th} \text{ degree of freedom}$$

The entries in the inertia matrix are:

$$m_{\gamma\gamma} = I_\gamma + 2S^2 I_b + 2C^2 I_{b_{long}} + 2m_b\left(d^2 + 2e^2 S^2 + 2eC_b S^2 + 2dC_b\beta_0\right)$$

$$m_{\gamma\phi} = m_{\phi\gamma} = 2SI_b + SI_{h_{lat}} + 2m_b\left(e^2 S + 2eC_b S + dC_b\beta_0 S\right)$$

$$m_{\gamma\beta_1} = m_{\beta_1\gamma} = -m_{\beta_2\gamma} = SI_b + m_b\left(eSC_b + dSC_b\beta_0\right) = -m_{\gamma\beta_2}$$

$$m_{\phi\phi} = 2I_b + I_{h_{lat}} + m_b\left(2e^2 + 4eC_b\right)$$

$$m_{\phi\beta_1} = -m_{\phi\beta_2} = m_{\beta_1\phi} = -m_{\beta_2\phi} = I_b + eC_b m_b$$

$$m_{\beta_1\beta_1} = m_{\beta_2\beta_2} = I_b$$

The entries in the gyroscopic/damping matrix are:

$$g_{\gamma\gamma} = 2\sin 2\psi\left(I_b - I_{b_{long}} + e^2 m_b + 2eC_b m_b\right) + \bar{c}_\gamma / \Omega$$

$$g_{\gamma\phi} = C\left(2I_{b_{long}} + 2I_{h_{lat}} - I_{h_{long}} + 4dC_b\beta_0 m_b\right)$$

$$g_{\gamma\beta_1} = -g_{\gamma\beta_2} = C\left(I_{b_{long}} + 2dC_b\beta_0 m_b\right)$$

$$g_{\phi\gamma} = C\left(4I_b - 2I_{b_{long}} + I_{h_{long}} + 4e^2 m_b + 8eC_b m_b\right)$$

$$g_{\phi\phi} = \bar{c}_\phi / \Omega$$

$$g_{\beta_1\gamma} = -g_{\beta_2\gamma} = C\left(2I_b - I_{b_{long}} + 2eC_b m_b\right)$$

$$g_{\beta_k\beta_k} = \bar{c}_{\beta_k} / \Omega; \quad k = 1,2$$

The entries in the stiffness matrix are:

$$k_{\gamma\gamma} = \frac{\bar{k}_\gamma}{\Omega^2}$$

$$k_{\gamma\phi} = S\left\{2I_b - I_{b_{long}} - I_{h_{lat}} + I_{h_{long}} + m_b\left(2e^2 + 4eC_b - 2dC_b\beta_0\right)\right\}$$

$$k_{\gamma\beta_1} = -k_{\gamma\beta_2} = S\left\{I_b - I_{b_{long}} + m_b\left(eC_b - dC_b\beta_0\right)\right\}$$

$$k_{\phi\phi} = 2I_b + 2I_{b_{long}} - I_{h_{lat}} + I_{h_{long}} + 2e^2 m_b + 4eC_b m_b + \frac{\bar{k}_\phi}{\Omega^2}$$

$$k_{\phi\beta_1} = k_{\beta_1\phi} = I_b - I_{b_{long}} + m_b C_b\left(e - \frac{gC}{\Omega^2}\right)$$

$$k_{\phi\beta_2} = k_{\beta_2\phi} = -I_b + I_{b_{long}} - m_b C_b\left(e + \frac{gC}{\Omega^2}\right)$$

$$k_{\beta_1\beta_1} = I_b - I_{b_{long}} + m_b C_b\left(e - \frac{gC}{\Omega^2}\right) + \frac{\bar{k}_{\beta_1}}{\Omega^2}$$

$$k_{\beta_2\beta_2} = I_b - I_{b_{long}} + m_b C_b\left(e + \frac{gC}{\Omega^2}\right) + \frac{\bar{k}_{\beta_2}}{\Omega^2}$$